RSC Advances

PAPER

View Article Online
View Journal | View Issue



Cite this: *RSC Adv.*, 2022, **12**, 23379

# Tyndall-effect-based colorimetric assay with colloidal silver nanoparticles for quantitative point-of-care detection of creatinine using a laser pointer pen and a smartphone†

Kaijing Yuan, Yao Sun, Fenchun Liang, Fenglan Pan, Miao Hu, Fei Hua, Yali Yuan, * Jinfang Nie* and Yun Zhang *

Herein, this paper initially reports a new colorimetric Tyndall effect-inspired assay (TEA) for simple, low-cost, sensitive, specific, and point-of-care detection of creatinine (an important small biomolecule) by making use of silver nanoparticles (AgNPs) as model colloidal nanoprobes for visual light scattering signaling. The naked-eye TEA method adopts negatively-charged citrate-capped AgNPs (Cit-AgNPs) prepared by sodium citrate reduction. In the presence of alkaline conditions, the creatinine analyte can form carbanion/oxoanion amino tautomers which in turn crosslink with carboxylate groups on the Cit-AgNPs *via* a hydrogen bonding network to mediate the aggregation of such colloidal nanoprobes showing a significantly-enhanced TE signal that was created and quantified by a hand-held laser pointer pen and a smartphone, respectively. The results demonstrate that the resulting equipment-free method with the TE readout could enable the portable quantification of creatinine with a detection limit of ~55 nM, which was ~90–2334 times lower than that obtained from AgNP-based colorimetric approaches with the most common localized surface plasma resonance signaling. Moreover, it shows a larger analytical sensitivity up to ~580.8227 signal per nM, offering ~2.4–232-fold improvement in comparison with many of the recent instrumental creatinine nanosensors. The accuracy and practicality of the developed nanosensing system was additionally confirmed with satisfactory recovery results ranging from *ca.* 98.52 to 100.36% when analyzing a set of real complex human urine samples.

Received 10th June 2022
Accepted 1st August 2022

DOI: 10.1039/d2ra03598g

rsc.li/rsc-advances



## 1. Introduction

Creatinine, a metabolite of creatine and final product of nitrogen metabolism in the human body, is filtered by the kidneys and excreted in urine.[1] Its concentration in human blood or urine plays an important role in assessing renal function and muscle damage clinically.[2–4] The creatinine concentrations higher than 170 μM can cause renal dysfunction,[5] while its level being lower than 70 μM implies decreased muscle weight that is related with muscle disorders.[6,7] The analytical toolbox available for creatinine detection mainly includes the traditional techniques such as Jaffé method,[8,9] UV-vis spectrophotometry,[10] high-performance liquid chromatography,[11] liquid chromatography with isotope-dilution mass spectrometry,[12] infrared spectroscopy,[13] capillary zone electrophoresis,[14,15] and nuclear magnetic resonance,[16] and recently-reported approaches like electrochemical sensors,[17,18] surface-enhanced Raman spectroscopy[19] and fluorescence assay.[6] Although most of these methods are highly sensitive and specific, they still suffer from the need for costly reagents and instruments, involve complicated sample pre-treatment, and are not suitable for point-of-care testing uses.[20–22]

In order to circumvent these issues, some efforts have been devoted alternatively to the development of colorimetric approaches with merits including simpler operation and less instrument investment for the creatinine sensing.[23] In recent years, colorimetric nanosensors with colloidal nanoparticles (primarily gold nanoparticles (AuNPs) and silver nanoparticles (AgNPs)) have received considerable attention because of their facile synthesis with tunable size and shape, robust nature, high surface-to-volume ratio, and excellent biocompatibility.[24–27] In particular, the colloidal AuNPs and AgNPs show distinctive chemical, physical, and distance-dependent optical properties, namely the localized surface plasmon resonance (LSPR) which can be easily observed by the naked eye.[25] In this regard, several efficient assays have been designed recently by functionalizing various creatinine-specific recognition molecules onto such nanoparticles, such as calix arene,[28] citrate,[2] 2,2-thiodiacetic

*Guangxi Key Laboratory of Electrochemical and Magnetochemical Function Materials, College of Chemistry and Bioengineering, Guilin University of Technology, 12 Jiangan Road, Guilin 541004, P. R. China. E-mail: zy@glut.edu.cn; Niejinfang@glut.edu.cn; thankSIN2013@163.com*

† Electronic supplementary information (ESI) available. See https://doi.org/10.1039/d2ra03598g

acid,[21] picric acid,[8,29] or sodium gluconate.[30] The analyte typically triggers the AuNPs' or AgNPs' LSPR-related red-to-blue or yellow-to-green (or yellow-to-purple) color change in the reaction solution which allows for rapid "yes or no" qualitative analysis. However, the LSPR-based colorimetric signaling still suffers from unsatisfactory visually-distinguishing ability and the requirement of expensive desktop equipment like UV-vis spectrometer to realize quantitative determination.[31] To response these challenges, more recently, our group has used the Tyndall effect (TE) of colloidal AuNPs to demonstrate an alternative approach for highly sensitive, low-cost and equipment-free quantification of metal ions including $Ag^{+}$,[32] small biomolecules like cocaine[33] and glutathione,[34] and interferon-γ protein marker[33] with significantly enhanced colorimetric signaling efficiency. The TE, one of basic optical features of a colloid which is named for the 19th-century British physicist John Tyndall, generally indicates a "visible light path" originated from the scattering of a light beam by the colloidal nanoparticles.[33,35] The TE intensity positively relies on either colloidal particles' size or concentration. In comparison, the AgNPs are actually preferred to the AuNPs of the same size due to their lower material cost and so on.[36] We also proposed an AgNP-based TE-inspired assay (TEA) for $Hg^{2+}$ detection.[37] However, it could only work based on the mechanism of the analyte-mediated nanoprobes' degradation, which was thus highly limited to be widely extended for the analysis of other sorts of targets of interest.

With these insights, in this proof-of-concept study, we describe a versatile TEA using the AgNP probes for single-step, sensitive, specific, colorimetric detection and portable quantification of creatinine (model analyte) in both artificial buffer samples and real human urine samples. Its working principle was schematically illustrated in Fig. 1. The citrate-capped AgNPs (Cit-AgNPs) are synthesized *via* hydrothermal reduction. The corresponding colloidal solution (with a set particle level) shows a quite weak TE response after it is illuminated using a 635 nm red laser pointer pen (hand-held light source). Upon the introduction of a creatinine sample, the aggregation of negatively-charged Cit-AgNPs would take place through an intermolecular hydrogen bonding network after the tautomerization of creatinine to its amino anionic species (carbanion/oxoanion) at the alkaline condition (pH ≈ 10.5),[38] leading to an enhanced TE signal. The degree of the TE enhancement is directly proportional to the analyte concentration in the sample. The naked-eye changes in the TE intensity enable the simple qualitative or semi-quantitative detection of creatinine levels. Portable quantitative detection can be additionally realized by using a smartphone for the TE readout. The main experimental factors have been optimized in details, including AgNP concentration, NaOH concentration, and reaction time and temperature. Under the optimal conditions, a detection limit of ~55 nM was achieved for the creatinine analyte, with an analytical sensitivity up to 580.8227 signal per nM which is ~232-times higher than that obtained from the common methods with the LSPR signaling and UV-vis spectrometer readers. Moreover, the proposed TEA approach holds great potential to be directly extended to all available AgNP-based colorimetric assays based on target-triggered probes' aggregation or dis-aggregation for the analysis of a broad spectrum of analytes ranging from metal ions,[32] small molecules,[39,40] to proteins[41] and cancer cells,[42] *etc.*

## 2. Experimental

### 2.1 Reagents and apparatus

Creatinine, ascorbic acid, cysteine (Cys), alanine (Ala), arginine (Arg), glycine (Gly), histidine (His), proline (Pro), serine (Ser),

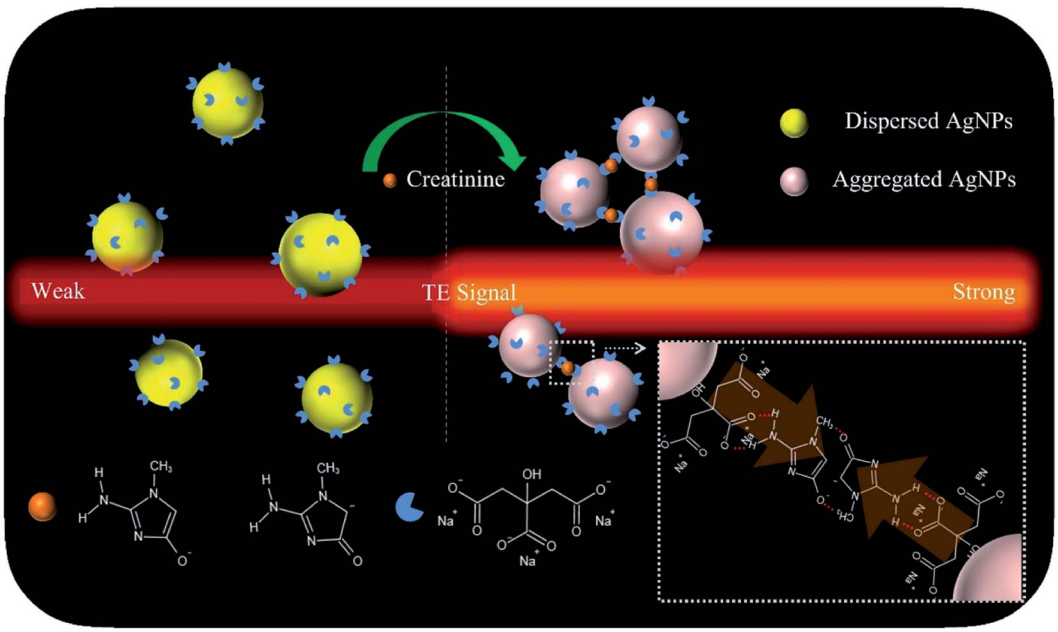


Fig. 1 Schematic representation of the sensing principle of the proposed TEA method with colloidal AgNP nanoprobes for the visual creatinine detection.

lysine (Lys), glutamic acid (Glu), tyrosine (Tyr), tryptophan (Trp), and valine (Val) were obtained from Sangon Biotechnology Co., Ltd. (Shanghai, China). Sodium citrate tribasic dehydrate was from Shanghai Biochemical Sci-Tech Co., Ltd. (Shanghai, China). Silver nitrate and sodium hydroxide (NaOH) were the products of Xilong Chemical Co., Ltd. (Guangzhou, China). All other chemicals were of analytical grade and used as received without further purification. All stock solutions were prepared with deionized water (with a specific resistivity $\geq$ 18.2 MΩ cm) produced using an ultrapure water equipment (UPS-II-20L) of Chengdu Yuechun Technology Co., Ltd. (Chengdu, China).

Hydrophilic polycarbonate nanoporous membranes (Whatman, ~50 nm in average pore size) were acquired from GE Healthcare Life Sciences. The human urine samples were obtained from our university hospital and filtrated with the polycarbonate membranes to remove potential interferences before their analysis (informed consent was obtained from all human subjects).

Optical characterization of dispersed and aggregated Cit-AgNPs was conducted using a UV-vis spectrometer (Cary 50, Varian, USA). Their morphology characterization was performed on a transmission electron microscope (TEM, JEM-2100F, JEOL, Japan). Fourier transform infrared (FTIR) spectra were recorded with a NicoletiS10 spectrometer (Thermo, USA). The TE signals were created with the aid of a 635 nm red laser pointer pen (5 mW; handheld light source) that was the product of Deli Group Co., Ltd. (Ningbo, China). All of the colorimetric results were recorded with a smartphone.

### 2.2 Synthesis of Cit-AgNPs

The Cit-AgNPs were synthesized according to a previous method[43] with a slight modification in which ascorbic acid and trisodium citrate were used as the reducing agent and the stabilizing reagent, respectively. In brief, an aqueous mixture was prepared by mixing 4 mL of 120 mM ascorbic acid and 4 mL of 6 mM trisodium citrate; its pH was further adjusted to 10.5 with 100 mM NaOH. Then, 80 μL of 100 mM silver nitrate was immediately added to this colorless solution under gentle, continuous stirring at 30 °C for 15 min, finally producing a yellow mixture containing Cit-AgNPs (2.8 nM). After allowing it to be cooled to room temperature, the Cit-AgNP solution was stored at 4 °C for further use. It was experimentally found that the freshly-prepared Cit-AgNPs may remain stable, with no significant change in creatinine sensing, for at least 6 months.

### 2.3 Creatinine detection with the common method

For the common method with the LSPR signaling, 10 μL of 600 mM NaOH solution, 480 μL of the freshly-prepared yellow Cit-AgNP solution (2.8 nM/0.7 nM) and 100 μL of creatinine sample were mixed successively and were incubated for 30 min at room temperature (25 °C). The color of the reaction mixture would change from yellow to purple or red due to the creatinine-induced Cit-AgNPs' aggregation, which allowed for visible qualitative or semi-quantitative creatinine analysis. Then, the absorption spectrum in the range of 300–800 nm was recorded for each reaction solution on an UV-vis spectrophotometer for quantitative measurement of creatinine levels.

### 2.4 Creatinine detection with the new method

For the new TEA method, the same mixing procedures above were carried out, except using 480 μL of 0.7 nM Cit-AgNP and each of the resultant reaction mixtures was illuminated using a red laser pointer pen (635 nm, 5 mW) to create a visual-TE signal for simple qualitative or semi-quantitative analysis. Moreover, each TE image was also recorded with a smartphone for further quantitative measurement of creatinine level. The TE intensity was defined as the average gray value (AG) of the corresponding image which was measured with the aid of the gray analysis option in Image J processing software. Then, the change of AG (ΔAG) for each creatinine sample was calculated from the following equation: $\Delta AG = AG_{creatinine} - AG_{blank}$, where $AG_{creatinine}$ and $AG_{blank}$ were obtained from a creatinine sample and the blank sample (without the analyte), respectively. Specificity (selectivity) experiments were performed in the same manner but using other 12 types of amino acids instead of the creatinine analyte, *i.e.*, the Lys, Tyr, Gly, Pro, Val, Ala, His, Glu, Arg, Ser, Trp and Cys.

## 3. Results and discussion

First, the feasibility of our new TEA method was demonstrated. As displayed in Fig. 2A, the colloidal Cit-AgNP solution appears a semitransparent and homogeneous yellow color (image a); its characteristic LSPR-related absorption peaks at ~400 nm in the corresponding UV-vis spectrum (black curve a).[31] From its corresponding TEM image (Fig. 2B, image a), most of the Cit-AgNPs contained in the solution are monodisperse, have relatively uniform spherical microstructures, and represent an average particle size estimated of *ca.* 50 nm. Since these colloidal nanoparticles are able to effectively scatter the light of the 635 nm laser, a clear red TE response can be observed in this colloid (Fig. 2B, inset of image a). On the other hand, upon the addition of 5 μM creatinine into the Cit-AgNP solution, the color of the resulting mixture changed from yellow to pink (Fig. 2A, image b), indirectly implying the aggregation of these nanoparticle probes due to intermolecular hydrogen bonding network formed between the analyte's carbanion/oxoanion amino tautomers (produced in the alkaline environment) and the exposed negatively-charged carboxylate groups of the citrate molecules. The formation of the hydrogen bonding was additionally confirmed by the Cit-AgNPs' FTIR spectra before and after the creatinine reaction (Fig. S1 in the ESI†).[44,45] The creatinine molecules contain free $NH_2$, and their N–H stretching frequency appears between 3300–3500 $cm^{-1}$. For the Cit-AgNPs, the peak variation around 3424 $cm^{-1}$ can be attributed to the stretching vibration of O–H. The peak variation at 3385 $cm^{-1}$ after the addition of creatinine to Cit-AgNPs is due to the overlapping stretching vibration of –N–H and O–H, where the stretching moves to higher frequencies. The peak becomes wider and smoother, which is attributed to the formation of hydrogen bonds between Cit-AgNPs and creatinine. The peak

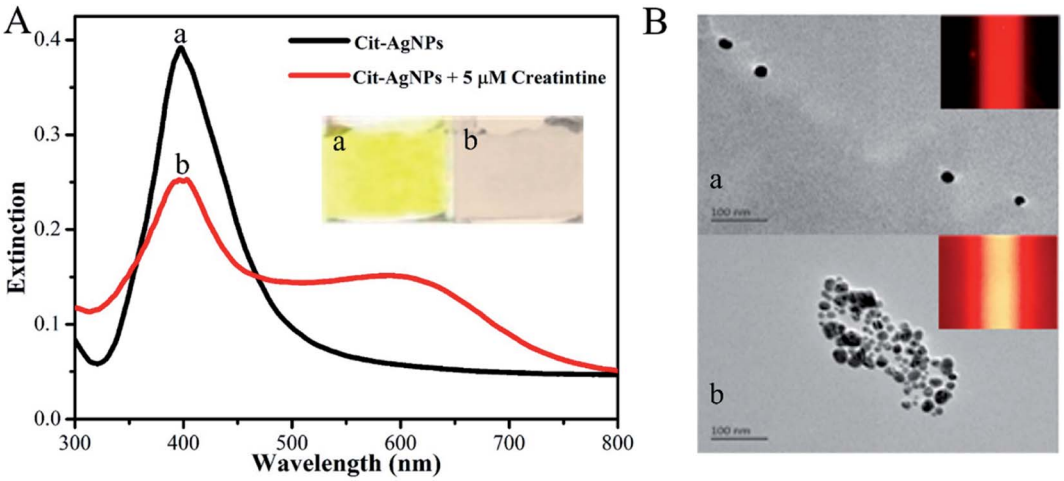


Fig. 2 (A) UV-vis spectra and (B) TEM images recorded from the Cit-AgNP solution (a) and the reaction mixture of the Cit-AgNPs and creatinine sample (5 μM) (b). Insets in (A) and (B) show the colorimetric results and TE results of the above two solutions, respectively.

around 2823 $cm^{-1}$ is the C–H stretching vibration, while the change in the peak around 1590 $cm^{-1}$ is due to the C=O stretching of the carboxyl group and the –N–H bending vibration of the amino group, apparently, the absorption band appearing at 1352 $cm^{-1}$ shows the C–H internal bending vibration of AgNPs. Its TEM image further offers direct evidence of the aggregated Cit-AgNPs (Fig. 2B, image b). The mixture solution was additionally characterized by its UV-vis spectrum, in which the remarkable decrease in the LSPR-related extinction centered at about 400 nm reflected a reduction in the level of the monodisperse Cit-AgNPs, while the red-shift in the LSPR band to around 600 nm reflected the increase in their particle size because of the aggregation reaction (Fig. 2A, red curve).[31] More importantly, it was interestingly found that compared with the initial solution, the creatinine-triggered Cit-AgNPs' aggregation led to a dramatically-enhanced TE signal (even with a yellow light path; Fig. 2B, inset of image b), presumably attributed to the higher light scattering efficiency of the colloidal particles' aggregates.

After demonstrating the sensing mechanism of the proposed new TEA approach, main experimental factors were then optimized to obtain the best signal-to-background ratio for the creatinine detection, including AgNP concentration, NaOH concentration, and reaction time and temperature (Fig. S2–S5 in ESI†). It was experimentally found that an assay run for the creatinine could be completed within 30 min at room temperature (25 °C) with 0.7 nM Cit-AgNP and 600 mM NaOH. Under such optimal conditions, a series of artificial creatinine samples with different levels ranging from 0 to 3200 nM were analyzed to evaluate the analytical performance and advantages of the TE-based signaling strategy, comparing with the results obtained from the LSPR-based conventional method with UV-vis spectroscopy measurement in which the freshly-prepared initial yellow Cit-AgNP solutions (*ca.* 2.8 nM) were adopted.

For the traditional method with the LSPR signaling, as shown in Fig. 3A, the creatinine-induced aggregation of Cit-AgNPs led to various color changes of the resultant reaction solutions from yellow to pink when the tested analyte level increased from 0 to 3200 nM. The visual limit of detection (V-LOD) for the analyte was estimated to be 2700 nM (Fig. 3A, image 6), which allowed for the formation of a reaction mixture showing a light–dark yellow color that was clearly distinguishable from that obtained from the blank sample (Fig. 3A, image 1). However, most solution colors of these mixtures cannot be visually distinguished from each other during the low concentration range of 0–2600 nM. Moreover, UV-vis spectra were measured for these reaction mixtures, with results displayed in Fig. 3C. One can see that since larger creatinine levels could lead to higher degrees of Cit-AgNPs' aggregation, the increase in the analyte concentration enabled the gradual decrease in the extinction peak at 400 nm in addition to the continuous increase in the extinction intensity at around 600 nm. As additionally shown in Fig. 3D (blue curve), the ratios of extinction values recorded at 600 and 400 nm ($E_{600}/E_{400}$) were linear over a creatinine concentration range of 2700–3000 nM. The quantitative LOD was calculated to be ~2600 nM according to the $3\sigma$ rule, defined as the concentration at the mean ($3\sigma$) of several determinations (here, 3 determinations) of the blank calibration.

For the new TEA method, on the other hand, the same analytical procedures above were carried out (except using 480 μL of 0.7 nM Cit-AgNP), which results shown in Fig. 3B. Most solution colors of these resulting reaction mixtures cannot be clearly distinguished from each other until the analyte level increased to 2800 nM (Fig. 3B, top, image 7), namely the V-LOD obtained with the low level of Cit-AgNP nanoprobes. Moreover, no meaningful changes were observed in the absorbance measured in their corresponding UV-vis spectra (Fig. 3C, inset). However, interestedly, after these reaction mixtures were further stimulated with a 635 nm red laser pen, almost all of the red scattering signals recorded from these different creatinine samples could be visually differentiated *via* the target-dependent TE responses (Fig. 3B, bottom). Stronger TE signals were generated at larger analyte levels which resulted in

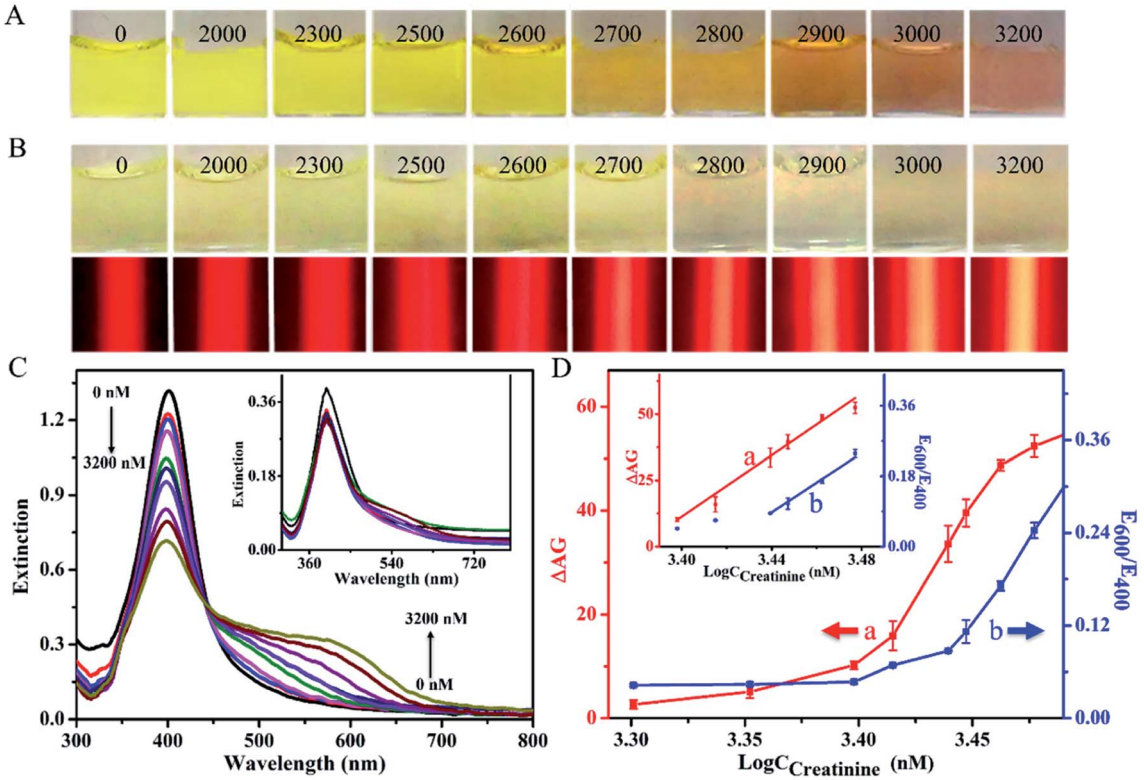


Fig. 3 (A) LSPR-based colorimetric results obtained from the traditional method for assaying different creatinine samples containing analyte concentrations from 0 to 3200 nM with freshly-prepared Cit-AgNPs (2.8 nM). (B) Colorimetric (top) and TE (bottom) results measured from the detection of the same creatinine samples above but using 0.7 nM Cit-AgNP as the sensing probes. (C) UV-vis spectra recorded from the mixtures shown in (A). Inset displays the UV-vis spectra of the mixtures shown in (B, top). (D) Calibration curves describing the relationships between the AG changes (△AG, red dot curve a) of the TE results shown in (B) or the ratio of the extinction values recorded at 600 and 400 nm ($E_{600}/E_{400}$) in the spectra (blue dot curve b) and the creatinine concentrations. Inset shows the relationships between the two types of signals and the analyte levels in two linear ranges. Each error bar represents a standard deviation across three replicate experiments.

the aggregation of more Cit-AgNP nanoprobes. These results confirmed that the TE of the Cit-AgNPs was able to offer a more ideal colorimetric signaling efficiency than their LSPR mechanism for naked-eye analysis. By comparing the assay of blank sample (Fig. 3B, above, image 1), the V-LOD of the new TE-based method for creatinine was defined as 2000 nM (Fig. 3B, above, image 2). Fig. 3D further shows the calibration curve where the ΔAG ($AG_{Creatinine} - AG_{blank}$) values were plotted as a function of creatinine concentration ($C_{Creatinine}$). The ΔAG value was positively linear to the analyte level over a range from 2500 to 3000 nM. The quantitative LOD was estimated to be as low as ~55 nM ($3\sigma$) which was ~47 times lower than that achieved by the common LSPR signaling method (*i.e.*, 2600 nM). In addition, compared to many other recent LSPR-based nanosensing techniques, the developed new equipment-free TEA system offered a *ca.* 90 to 2334-fold increase in the analytical sensitivity (defined as the slope of the corresponding regression equation) without the use of any bulky equipment like UV-vis spectrometer, surface enhanced Raman spectrometer, or fluorescence spectrometer, but just a cheap laser pointer pen and a ubiquitous smartphone (Table S1†).

Next, the analytical specificity of our nanosensor was evaluated as another key performance factor by parallelly analyzing a blank sample (with no analyte), 5 μM creatinine, and other 12 types of amino acids (*i.e.*, Lys, Tyr, Gly, Pro, Val, Ala, His, Glu, Arg, Ser, Trp, and Cys; 1000 μM each) under the same optimal experimental conditions. Fig. 4A displays that the reaction solution from the creatinine sample shows a clear light pink color because of the aggregated Cit-AgNPs involved. And no significant changes in the mixtures' yellow color can be observed between the assays of the blank sample and other 12 types of amino acids which should show no significant effect on the nanoprobes' dispersion (Fig. 4B). Accordingly, quite similar weak red TE responses were produced for either the blank sample or the 12 cases of non-specific small molecules, leading to almost the same low AG values of about 50 showed in Fig. 4C. However, as expected, only the creatinine analysis resulted in the production of a very strong TE signal and a big AG value up to *ca.* 120 (Fig. 4C). These results clearly demonstrated that only the analyte had formed amino interconversion isomers in the alkaline environment to crosslink with the negatively charged citrate caps on the surfaces of the Cit-AgNP probes for triggering their subsequent serious aggregation, thus endowing the designed sensing method with desirable high specificity (selectivity).

Finally, the practicality of this new Cit-AgNP-based TEA nanosensor was studied by analyzing creatinine in several human urine samples collected from healthy volunteers. Three

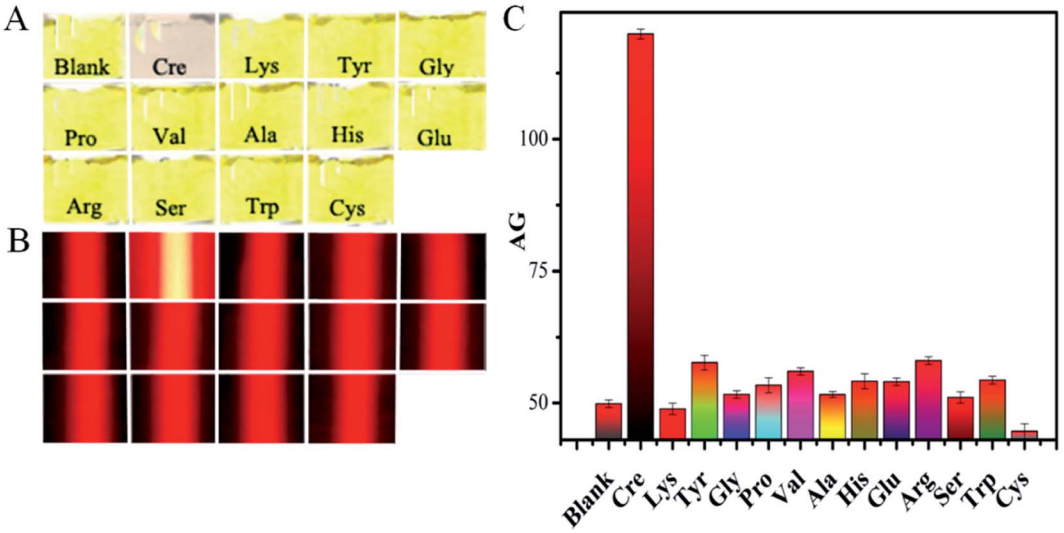


Fig. 4 (A) Colorimetric results and (B) TE images measured from blank sample (without the analyte), 5 μM creatinine sample, and other 12 sorts of amino acids (1000 μM each). (C) The corresponding AG values calculated from the TE signals shown in (B). Each error bar is the standard deviation of three repeated parallel experiments.

Table 1 Recovery of creatinine in human urine samples

| Sample | Found (nM) | Added (nM) | Total found (nM) | Recovery (%) | RSD[b] (%, $n = 3$) |
|---|---|---|---|---|---|
| Human urine[a] | 0.00 | 2500 | 2510 | 100.36 | 2.85 |
| | 0.00 | 2800 | 2760 | 98.78 | 1.10 |
| | 0.00 | 3000 | 2960 | 98.52 | 3.99 |

[a] Human urine was diluted 10 000 times before analysis. [b] RSD, relative standard deviation.

parallel experiments were performed for each sample according to the normal analytical procedures. As summarized in Table 1, the recovery results obtained range from 98.52 to 100.36% with the relative standard deviations (RSDs) in a range of 1.10–3.99%. Such acceptable recoveries and small RSDs indicate the relatively high accuracy and practicality of the developed method for the analysis of real complex samples like human body fluids.

## 4. Conclusions

We have developed successfully a new portable nanosensor with a laser pointer pen and a smartphone for the naked-eye detection of creatinine in human urine by taking the advantages of colloidal Cit-AgNPs and their TE for highly efficient colorimetric signaling. This TEA system was based on the analyte-triggered aggregation and subsequent TE enhancement of these light scattering probes *via* an intramolecular hydrogen bonding network that was formed between the carboxylate groups on their surfaces and the carbanion and oxoanion amino tautomers of the tested small molecules generated in an alkaline condition. The results demonstrated well that such equipment-free TE-based method could not only offer a ~50-fold improvement in the colorimetric signaling efficiency in comparison with the most commonly applied LSPR strategy, but also achieve a high detection sensitivity which was ~2.4–232 times larger than that obtained from many of recently-reported instrumental assays with various large sophisticated equipment such as UV-vis spectrometer. We believe that the proposed method holds a great promise to be further tailored to expend to all available colorimetric assays with the AgNPs based on the analyte-induced probes' aggregation or dis-aggregation for point-of-use analysis of metal ions,[32] small molecules,[39,40] proteins[41] or even cancer cells[42] especially in a variety of resource-poor settings like home healthcare and on-site environmental pollution monitoring.

## Conflicts of interest

The authors declare no competing flnancial interest.

## Acknowledgements

This work was financially supported by National Natural Science Foundation of China (No. 21874032, 21765007 and 21765005), Guangxi Science Fund for Distinguished Young Scholars (No. 2018GXNSFFA281002), and Central Government-Guided Local Science and Technology Development Project (No. GuikeZY20198006).

## References

1 R. Narimani, M. Azizi, M. Esmaeili, S. H. Rasta and H. T. Khosroshahi, An optimal method for measuring biomarkers: colorimetric optical image processing for determination of creatinine concentration using silver nanoparticles, *3 Biotech*, 2020, **10**(10), 416.

2 Y. Xia, C. Zhu, J. Bian, Y. Li, X. Liu and Y. Liu, Highly sensitive and selective colorimetric detection of creatinine based on synergistic effect of PEG/Hg(2+)-AuNPs, *Nanomaterials*, 2019, **9**(10), 1024.

3 J. Sittiwong and F. Unob, Detection of urinary creatinine using gold nanoparticles after solid phase extraction, *Spectrochim. Acta Mol. Biomol. Spectrosc.*, 2015, **138**, 381–386.

4 W. R. de Araújo, M. O. Salles and T. R. L. C. Paixao, Development of an enzymeless electroanalytical method for the indirect detection of creatinine in urine samples, *Sens. Actuators, B*, 2012, **173**, 847–851.

5 C. S. Pundir, P. Kumar and R. Jaiwal, Biosensing methods for determination of creatinine: a review, *Biosens. Bioelectron.*, 2019, **126**, 707–724.

6 R. Rajamanikandan and M. Ilanchelian, Protein-protected red emittive copper nanoclusters as a fluorometric probe for highly sensitive biosensing of creatinine, *Anal. Methods*, 2018, **10**(29), 3666–3674.

7 N. Chauhan, J. Narang, Shweta and C. S. Pundir, Immobilization of barley oxalate oxidase onto gold-nanoparticle-porous $CaCO_3$ microsphere hybrid for amperometric determination of oxalate in biological materials, *Clin. Biochem.*, 2012, **45**(3), 253–258.

8 A. K. Parmar, N. N. Valand, K. B. Solanki and S. Menon, Picric acid capped silver nanoparticles as a probe for colorimetric sensing of creatinine in human blood and cerebrospinal fluid samples, *Analyst*, 2016, **4**, 1488–1498.

9 M. Jaffe, Ueber den Niederschlag, welchen Pikrinsure in normalem Harn erzeugt und über eine neue Reaction des Kreatinins, *Biol. Chem.*, 1886, **10**(5), 391–400.

10 D. C. Gloria, I. Ana and C. J. Alfonso, Spectrophotometric simultaneous determination of creatinine and creatine by flow injection with reagent injection, *Fresenius. J. Anal. Chem.*, 1995, **352**(1995), 557–561.

11 Y. D. Yang, Simultaneous determination of creatine, uric acid, creatinine and hippuric acid in urine by high performance liquid chromatography, *BMC*, 1998, **12**(2), 47–49.

12 R. Harlan, W. Clarke, J. M. Di Bussolo, M. Kozak, J. Straseski and D. L. Meany, An automated turbulent flow liquid chromatography-isotope dilution mass spectrometry (LC-IDMS) method for quantitation of serum creatinine, *Clin. Chim. Acta*, 2010, **411**(21–22), 1728–1734.

13 J. L. Pezzaniti, T. W. Jeng, L. McDowell and G. Oosta, Preliminary investigation of near-infrared spectroscopic measurements of urea, creatinine, glucose, protein, and ketone in urine, *Clin. Biochem.*, 2001, **34**(3), 239–246.

14 E. A. Clark, J. C. Fanguy and C. S. Henry, High-throughput multi-analyte screening for renal disease using capillary electrophoresis, *J. Pharmaceut. Biomed. Anal.*, 2001, **25**(5–6), 795–801.

15 A. C. Costa, J. L. da Costa, F. G. Tonin, M. F. Tavares and G. A. Micke, Development of a fast capillary electrophoresis method for determination of creatinine in urine samples, *J. Chromatogr., A*, 2007, **1171**(1–2), 140–143.

16 S. H. Choi, S. D. Lee, J. H. Shin, J. Ha and G. S. Cha, Amperometric biosensors employing an insoluble oxidant as an interference-removing agent, *Anal. Chim. Acta*, 2002, **461**(2), 251–260.

17 J.-C. Chen, A. S. Kumar, H.-H. Chung, S.-H. Chien, M.-C. Kuo and J.-M. Zen, An enzymeless electrochemical sensor for the selective determination of creatinine in human urine, *Sens. Actuators, B*, 2006, **115**(1), 473–480.

18 F. C. Wei, S. Korin, Y. Reed, E. F. Gjertson, D. Ho, C. M. Gritsch and H. A. Veale, Serum creatinine detection by a conducting-polymer-based electrochemical sensor to identify allograft dysfunction, *Anal. Chem.*, 2012, **84**(18), 7933–7937.

19 M. T. Alula and J. Yang, Photochemical decoration of magnetic composites with silver nanostructures for determination of creatinine in urine by surface-enhanced Raman spectroscopy, *Talanta*, 2014, **130**, 55–62.

20 Y. He, X. Zhang and H. Yu, Gold nanoparticles-based colorimetric and visual creatinine assay, *Microchim. Acta*, 2015, **182**(11), 2037–2043.

21 S. Mohammadi and G. Khayatian, Highly selective and sensitive photometric creatinine assay using silver nanoparticles, *Microchim. Acta*, 2015, **182**(7–8), 1379–1386.

22 M. Braiek, M. A. Djebbi, J. F. Chateaux, A. Bonhomme, R. Vargiolu, F. Bessueille and N. Jaffrezic-Renault, A conductometric creatinine biosensor prepared through contact printing of polyvinyl alcohol/polyethyleneimine based enzymatic membrane, *Microelectron. Eng.*, 2018, **187–188**, 43–49.

23 A. Dsc, B. Phw, B. Ych, B. Mcy, A. Syl and B. Cyl, Colorimetric and amperometric detection of urine creatinine based on the ABTS radical cation modified electrode, *Sens. Actuators, B*, 2020, **314**(2020), 128034.

24 E. Priyadarshini and N. Pradhan, Gold nanoparticles as efficient sensors in colorimetric detection of toxic metal ions: a review, *Sens. Actuators, B*, 2017, **238**(2017), 888–902.

25 F. Fathi, M. Rashidi and Y. Omidi, Ultra-sensitive detection by metal nanoparticles-mediated enhanced SPR biosensors, *Talanta*, 2018, **192**(2019), 118–127.

26 M. Hepel and M. Stobiecka, Detection of oxidative stress biomarkers using functional gold nanoparticles, *Fine Particles in Medicine and Pharmacy*, 2012, pp. 241–281.

27 S. Link and M. A. El-Sayed, Optical properties and ultrafast dynamics of metallic nanocrystals, *Annu. Rev. Phys. Chem.*, 2003, **54**(1), 331–366.

28 P. G. Sutariya, A. Pandya, A. Lodha and S. K. Menon, A simple and rapid creatinine sensing via DLS selectivity, using calix[4]arene thiol functionalized gold nanoparticles, *Talanta*, 2016, **147**, 590–597.

29 P. Falcó, L. Genaro, S. M. Lloret, F. B. Gomez and C. M. Legua, Creatinine determination in urine samples by

batchwise kinetic procedure and flow injection analysis using the Jaffé reaction: chemometric study, *Talanta*, 2001, **55**(6), 1079–1089.

30 S. Sadeghi and M. Hosseinpour, Sodium gluconate capped silver nanoparticles as a highly sensitive and selective colorimetric probe for the naked eye sensing of creatinine in human serum and urine, *Microchem. J.*, 2020, **154**(2020), 104601.

31 M. T. Alula, L. Karamchand, N. R. Hendricks and J. M. Blackburn, Citrate-capped silver nanoparticles as a probe for sensitive and selective colorimetric and spectrophotometric sensing of creatinine in human urine, *Anal. Chim. Acta*, 2018, **1007**, 40–49.

32 J. Yang, Y. Zhang, L. Zhang, H. Wang, J. Nie, Z. Qin, J. Li and W. Xiao, Analyte-triggered autocatalytic amplification combined with gold nanoparticle probes for colorimetric detection of heavy-metal ions, *Chem. Commun.*, 2017, **53**(54), 7477–7480.

33 W. Xiao, Z. Deng, J. Huang, Z. Huang, M. Zhuang, Y. Yuan, J. Nie and Y. Zhang, Highly sensitive colorimetric detection of a variety of analytes via the Tyndall Effect, *Anal. Chem.*, 2019, **91**(23), 15114–15122.

34 Y. Sun, K. Yuan, X. Mo, X. Chen, Y. Deng, C. Liu, Y. Yuan, J. Nie and Y. Zhang, Tyndall-Effect-inspired assay with gold nanoparticles for the colorimetric discrimination and quantification of mercury ions and glutathione, *Talanta*, 2022, **238**, 122999.

35 Z. Deng, W. Jin, Q. Yin, J. Huang, Z. Huang, H. Fu, Y. Yuan, J. Zou, J. Nie and Y. Zhang, Ultrasensitive visual detection of $Hg^{2+}$ ions via the Tyndall effect of gold nanoparticles, *Chem. Commun.*, 2021, **57**(21), 2613–2616.

36 M. Rycenga, C. M. Cobley, J. Zeng, W. Li, C. H. Moran, Q. Zhang, D. Qin and Y. Xia, Controlling the synthesis and assembly of silver nanostructures for plasmonic applications, *Chem. Rev.*, 2011, **111**(6), 3669–3712.

37 J. Huang, X. Mo, H. Fu, Y. Sun, Q. Gao, X. Chen, J. Zou, Y. Yuan, J. Nie and Y. Zhang, Tyndall-effect-enhanced supersensitive naked-eye determination of mercury (II) ions with silver nanoparticles, *Sens. Actuators, B*, 2021, **344**(2021), 130218.

38 A. M. E. Badawy, T. P. Luxton, R. G. Silva, K. G. Scheckel, M. T. Suidan and T. M. Tolaymat, Impact of environmental conditions (pH, ionic strength, and electrolyte type) on the surface charge and aggregation of silver nanoparticles suspensions, *Environ. Sci. Technol.*, 2010, **44**(4), 1260–1266.

39 X. Xu, J. W. Fan, Y. K. Jiao and X. Yang, Label-free colorimetric detection of small molecules utilizing DNA oligonucleotides and silver nanoparticles, *Small*, 2010, **5**(23), 2669–2672.

40 A. Kumar, G. Vyas, M. Bhatt, S. Bhatt and P. Paul, Silver nanoparticle based highly selective and sensitive solvatochromatic sensor for colorimetric detection of 1,4-dioxane in aqueous media, *Chem. Commun.*, 2015, **51**(2015), 15936.

41 C. Smsab, A. Bsm, D. Dgp and B. Dhka, A colorimetric alkaline phosphatase biosensor based on p -aminophenol-mediated growth of silver nanoparticles, *Colloids Surf. B Biointerfaces*, 2021, **205**(2021), 111835.

42 S. P. Singh, A. Mishra, R. K. Shyanti, R. P. Singh and A. Acharya, Silver nanoparticles synthesized using carica papaya Leaf extract (AgNPs-PLE) causes cell cycle arrest and apoptosis in human prostate (DU145) Cancer Cells, *Biol. Trace Elem. Res.*, 2021, **199**(2021), 1316–1331.

43 Y. Qin, X. Ji, J. Jing, H. Liu, H. Wu and W. Yang, Size control over spherical silver nanoparticles by ascorbic acid reduction, *Colloids Surf. A Physicochem. Eng. Asp.*, 2010, **372**(1–3), 172–176.

44 B. Banerji and S. K. Pramanik, Binding studies of creatinine and urea on iron-nanoparticle, *Springerplus*, 2015, **4**, 708.

45 L. C. Zhumei Sun, Y. Shua, Q. Li, M. Liu and D. Qiu, Chemical bond between chloride ions and surface carboxyl groups on activated carbon, *Colloids Surf., A*, 2017, **530**(2017), 53–59.